J|A|C|S
ARTICLES
Published on Web 01/31/2006

Quantum Dot Solar Cells. Harvesting Light Energy with CdSe Nanocrystals Molecularly Linked to Mesoscopic TiO_2 Films

István Robel,[†,||] Vaidyanathan Subramanian,[†,§] Masaru Kuno,*[,†,‡] and Prashant V. Kamat*[,†,‡,§]

Contribution from the Notre Dame Radiation Laboratory, Department of Chemistry and Biochemistry, Department of Chemical and Biomolecular Engineering, and Department of Physics, University of Notre Dame, Notre Dame, Indiana 46556-5674

Received September 21, 2005; E-mail: pkamat@nd.edu; mkuno@nd.edu

Abstract: By using bifunctional surface modifiers (SH−R−COOH), CdSe quantum dots (QDs) have been assembled onto mesoscopic TiO_2 films. Upon visible light excitation, CdSe QDs inject electrons into TiO_2 nanocrystallites. Femtosecond transient absorption as well as emission quenching experiments confirm the injection from the excited state of CdSe QDs into TiO_2 nanoparticles. Electron transfer from the thermally relaxed s-state occurs over a wide range of rate constant values between 7.3×10^9 and 1.95×10^{11} s^{-1}. The injected charge carriers in a CdSe-modified TiO_2 film can be collected at a conducting electrode to generate a photocurrent. The TiO_2−CdSe composite, when employed as a photoanode in a photoelectrochemical cell, exhibits a photon-to-charge carrier generation efficiency of 12%. Significant loss of electrons occurs due to scattering as well as charge recombination at TiO_2/CdSe interfaces and internal TiO_2 grain boundaries.

Introduction

Increasing demand for energy soon will force us to seek environmentally clean alternative energy resources.[1−3] Recent efforts to design ordered assemblies of semiconductor and metal nanoparticles as well as carbon nanostructures provide innovative strategies for designing next generation energy conversion devices.[4−9] Renewable energy such as solar radiation is ideal to meet the projected demand but requires new initiatives to harvest incident photons with higher efficiency, for example, by employing nanostructured semiconductors and molecular assemblies. Dye sensitization of mesoscopic TiO_2 has been widely used in this context. Power conversion efficiencies up to 11% have been achieved for such photochemical solar cells.[10−12] Semiconductors such as CdS,[13−15] PbS,[16,17] Bi_2S_3,[16,18] CdSe,[19] and InP,[20] which absorb light in the visible, can serve as sensitizers as they are able to transfer electrons to large band gap semiconductors such as TiO_2 or SnO_2.

Scheme 1. (a) Linking CdSe Quantum Dots to TiO_2 Particle with Bifunctional Surface Modifier; (b) Light Harvesting Assembly Composed of TiO_2 Film Functionalized with CdSe QDs on Optically Transparent Electrode (Not to Scale)

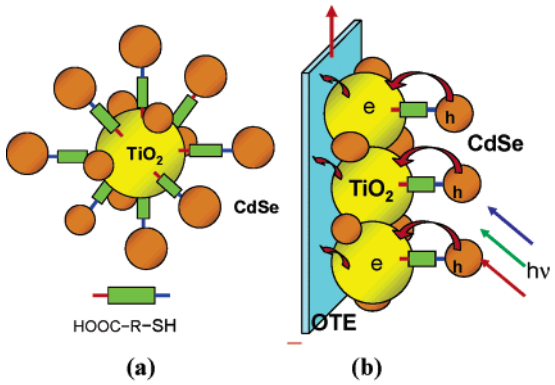

Semiconductor quantum dots (QDs) such as CdSe with its tunable band edge offer new opportunities for harvesting light

[†] Notre Dame Radiation Laboratory.
[‡] Department of Chemistry and Biochemistry.
[§] Department of Chemical and Biomolecular Engineering.
[||] Department of Physics.

(1) Lewis, N. S.; Crabtree, G. W.; Nozik, A. J.; Wasielewski, M. R.; Alivisatos, A. P. *Basic Energy Sciences Report on Basic Research Needs for Solar Energy Utilization*; Office of Science, U.S. Department of Energy, April 18−21, 2005: Washington, DC, 2005.
(2) Dresselhaus, M. S.; Thomas, I. L. *Nature* **2001**, *414*, 332−337.
(3) Crabtree, G. W.; Dresselhaus, M. S.; Buchanan, M. V. *Phys. Today* **2004**, *57*, 39−44.
(4) Kamat, P. V. *J. Phys. Chem. B* **2002**, *106*, 7729−7744.
(5) Adams, D.; et al. *J. Phys. Chem. B* **2003**, *107*, 6668−6697.
(6) George Thomas, K.; Kamat, P. V. *Acc. Chem. Res.* **2003**, *36*, 888−898.
(7) Shipway, A. N.; Katz, E.; Willner, I. *Chem. Phys. Chem.* **2000**, *1*, 18−52.
(8) Willner, I.; Kaganer, E.; Joselevich, E.; Durr, H.; David, E.; Gunter, M. J.; Johnston, M. R. *Coord. Chem. Rev.* **1998**, *171*, 261−285.
(9) Ward, M. D. *Chem. Soc. Rev.* **1999**, 365−375.
(10) Cahen, D.; Hodes, G.; Graetzel, M.; Guillemoles, J. F.; Riess, I. *J. Phys. Chem.* **2000**, *104*, 2053−2059.
(11) Graetzel, M. *Nature* **2001**, *414*, 338.
(12) Graetzel, M., Nanocrystalline electronic junctions. In *Semiconductor Nanoclusters − Physical, Chemical and Catalytic Aspects*; Kamat, P. V., Meisel, D., Eds.; Elsevier Science: Amsterdam, 1997; pp 353−375.
(13) Gerischer, H.; Luebke, M. *J. Electroanal. Chem.* **1986**, *204*, 225−7.
(14) Vogel, R.; Pohl, K.; Weller, H. *Chem. Phys. Lett.* **1990**, *174*, 241−6.
(15) Kohtani, S.; Kudo, A.; Sakata, T. *Chem. Phys. Lett.* **1993**, *206*, 166−70.
(16) Vogel, R.; Hoyer, P.; Weller, H. *J. Phys. Chem.* **1994**, *98*, 3183−3188.
(17) Plass, R.; Pelet, S.; Krueger, J.; Gratzel, M.; Bach, U. *J. Phys. Chem. B* **2002**, *106*, 7578−7580.
(18) Peter, L. M.; Wijayantha, K. G. U.; Riley, D. J.; Waggett, J. P. *J. Phys. Chem. B* **2003**, *107*, 8378−8381.
(19) Liu, D.; Kamat, P. V. *J. Phys. Chem.* **1993**, *97*, 10769−73.
(20) Zaban, A.; Micic, O. I.; Gregg, B. A.; Nozik, A. J. *Langmuir* **1998**, *14*, 3153−3156.

energy in the visible region of the solar spectrum.[21,22] Most studies reported to date have been limited to explorations of QD photophysical properties[23−26] or their use as biological probes.[27−30] Few recent studies report their use in organic photovoltaic cells.[31−33] The blend of polyphenylenevinylene (PPV) and CdSe QDs, for example, facilitates charge separation and the generation of photocurrents under visible light irradiation.

Ordered assemblies of narrow band gap semiconductor nanostructures are convenient systems by which to harvest visible light energy if employed as electrodes in photoelectrochemical cells. The photocurrent obtained using such nanoparticle assemblies is often low as fast charge recombination limits photocurrent generation. By employing composite semiconductors, however, it has been possible to improve the efficiency of charge separation through charge rectification.[34] Chemically and electrochemically deposited CdS and CdSe nanocrystallites are capable of injecting electrons into wider gap materials such as TiO_2,[13,35] SnO_2,[36,37] and ZnO,[38,39] generating photocurrents under visible light irradiation. Size quantization often becomes an important factor to drive the energetics to more favorable levels as in the case of TiO_2/PbS.[16]

Specific advantages of using semiconductor QDs as light harvesting assemblies in solar cells exist.[21] First and foremost, size quantization allows us to tune the visible response and vary the band offsets to modulate the vectorial charge transfer across different sized particles. In addition, these QDs open up new ways to utilize hot electrons[40] or generate multiple charge carriers with a single photon.[41] Impact ionization (or inverse Auger scattering) processes in PbSe nanocrystals have shown that two or more excitons can be generated with a single photon of energy greater than twice the band gap.[41−43] To explore the salient features of QDs, we have assembled TiO_2 and CdSe nanoparticles using bifunctional surface modifiers of the type HS−R−COOH (Scheme 1). Photochemical processes that follow the excitation of CdSe QDs, as probed by photoelectrochemical and transient absorption measurements, are presented.

Experimental Section

Materials. The precursors cadmium oxide (CdO, Aldrich), tetradecylphosphonic acid (TDPA, Avocado), trioctylphosphine oxide (TOPO, Aldrich), selenium (Aldrich), and trioctylphosphine (TOP, Aldrich) were used as supplied to prepare CdSe QDs. Mercaptopropionic acid (MPA), thiolacetic acid (TAA), and mercaptohexadecanoic acid (MDA) were also obtained from Aldrich. Titanium(IV) isopropoxide (Aldrich) serves as a precursor to prepare TiO_2 colloids. Conducting glass plates (1 × 5 cm), obtained from Pilkington, were used as optically transparent electrodes (OTE).

Preparation of CdSe Nanoparticles. A one-pot synthesis is used to create colloidal CdSe QDs.[44] In particular, 0.05 g (∼0.39 mmol) of CdO and 0.30 g (∼1.1 mmol) of TDPA are mixed in a ∼1:2−1:3 mole ratio with 4.0 g of TOPO. The mixture is heated under nitrogen at 320 °C to coordinate Cd ions with the phosphonic acid. Upon completion, the temperature is lowered to 270 °C, and 0.25 mL (1 M) TOPSe diluted with 4.0 mL of TOP is injected into the mixture. This causes the solution temperature to drop to ∼240−250 °C. Subsequent growth is carried out at 270 °C. On reaching the desired QD size, as determined through UV/visible spectroscopy,[45] the temperature is lowered, stopping the reaction.

CdSe Linked TiO_2 Colloidal Suspension for Spectroscopy Measurements. A solution of mercaptopropionic acid is added dropwise to a 50/50 THF/EtOH solution of CdSe nanoparticles. TiO_2 colloids are prepared by adding 0.25 mL of titanium isopropoxide (10% in *i*-PrOH) dropwise to 10 mL of ethanol under vigorous stirring. The two solutions are later mixed in a ratio of 1:25 TiO_2:CdSe by volume, allowing the hydrolyzed TiO_2 to bind to CdSe QDs through the linker molecules. The resulting solution is stirred for 2 h before being employed for spectroscopy measurements.

TiO_2/CdSe Films for Photoelectrochemical Measurements. TiO_2 colloids were first prepared by hydrolyzing titanium isopropoxide in a glacial acetic acid solution followed by autoclaving the suspension at 497 K for 12 h. The details of the procedure can be found elsewhere.[46] The suspension was sonicated whereupon a known amount was applied to the conducting glass plates (referred as OTE) and dried. After annealing these electrodes at 673 K, the weight of the film was determined. The average thickness of the film was subsequently determined from the weight, density, and area of the TiO_2 film. Thicker films were obtained by carrying out repeated applications of the TiO_2 suspension followed by drying.

The TiO_2 films, stored in an oven (∼373 K), were subsequently dipped into a solution of acetonitrile containing carboxy alkane thiols (TAA, MPA, and MDA). The films were kept immersed for ∼4 h. Resulting TiO_2 films, functionalized with these bifunctional surface modifiers, were then washed with both acetonitrile and toluene and transferred to a glass vial containing a suspension of CdSe QDs in toluene. The electrodes were kept immersed in the CdSe solution for approximately 12 h. Scheme 2 shows the sequence of steps followed. The resulting film is referred to as TiO_2/L/CdSe films (L = TAA, MPA, and MDA).

Optical and Electrochemical Measurements. Absorption spectra were recorded using a Shimadzu UV-3101 PC spectrophotometer. Emission spectra were recorded using a SLM-S 8000 spectrofluorimeter. Photoelectrochemical studies were carried out in a three-armed cell with a Pt-gauze counter electrode and a saturated calomel electrode (SCE) as a reference. An aqueous Na_2S solution serves as a redox

(21) Nozik, A. J. *Physica E* **2002**, *14*, 115−120.
(22) Wang, Z. L. *J. Phys. Chem.* **2000**, *104*, 1153−1175.
(23) Henglein, A. *Chem. Rev.* **1989**, *89*, 1861−73.
(24) Nirmal, M.; Brus, L. *Acc. Chem. Res.* **1999**, *32*, 407−414.
(25) Empedocles, S.; Bawendi, M. *Acc. Chem. Res.* **1999**, *32*, 389−396.
(26) Kuno, M.; Fromm, D. P.; Hamann, H. F.; Gallagher, A.; Nesbitt, D. J. *J. Chem. Phys.* **2000**, *112*, 3117−3120.
(27) Chan, W. C. W.; Nie, S. *Science* **1998**, *281*, 2016−2018.
(28) Mattoussi, H.; Mauro, J. M.; Goldman, E. R.; Anderson, G. P.; Sundar, V. C.; Mikulec, F. V.; Bawendi, M. G. *J. Am. Chem. Soc.* **2000**, *122*, 12142−12150.
(29) Niemeyer, C. M. *Angew. Chem., Int. Ed.* **2001**, *40*, 4128−4158.
(30) Bruchez, M.; Moronne, M.; Gin, P.; Weiss, S.; Alivisatos, A. P. *Science* **1998**, *281*, 2013−2016.
(31) Mattoussi, H.; Radzilowski, L. H.; Dabbousi, B. O.; Thomas, E. L.; Bawendi, M. G.; Rubner, M. F. *J. Appl. Phys.* **1998**, *83*, 7965−7974.
(32) Huynh, W. U.; Dittmer, J. J.; Alivisatos, A. P. *Science* **2002**, *295*, 2425−2427.
(33) Pientka, M.; Wisch, J.; Boger, S.; Parisi, J.; Dyakonov, V.; Rogach, A.; Talapin, D.; Weller, H. *Thin Solid Films* **2004**, *451−52*, 48−53.
(34) Liu, D.; Kamat, P. V. *J. Electroanal. Chem. Interfacial Electrochem.* **1993**, *347*, 451−6.
(35) Hao, E.; Yang, B.; Zhang, J.; Zhang, X.; Sun, J.; Shen, J. *J. Mater. Chem.* **1999**, *8*, 1327−1328.
(36) Nasr, C.; Kamat, P. V.; Hotchandani, S. *J. Electroanal. Chem.* **1997**, 420, 201−207.
(37) Nasr, C.; Hotchandani, S.; Kim, W. Y.; Schmehl, R. H.; Kamat, P. V. *J. Phys. Chem. B* **1997**, *101*, 7480−7487.
(38) Hotchandani, S.; Kamat, P. V. *Chem. Phys. Lett.* **1992**, *191*, 320−6.
(39) Hotchandani, S.; Kamat, P. V. *J. Phys. Chem.* **1992**, *96*, 6834−9.
(40) Ross, R. T.; Nozik, A. J. *J. Appl. Phys.* **1982**, *53*, 3813−8.
(41) Schaller, R. D.; Klimov, V. I. *Phys. Rev. Lett.* **2004**, *92*, 186601.
(42) Ellingson, R. J.; Beard, M. C.; Johnson, J. C.; Yu, P. R.; Micic, O. I.; Nozik, A. J.; Shabaev, A.; Efros, A. L. *Nano Lett.* **2005**, *5*, 865−871.
(43) Califano, M.; Zunger, A.; Franceschetti, A. *Nano Lett.* **2004**, *4*, 525−531.
(44) Peng, Z. A.; Peng, X. *J. Am. Chem. Soc.* **2001**, *123*, 183−184.
(45) Yu, W. W.; Qu, L. H.; Guo, W. Z.; Peng, X. G. *Chem. Mater.* **2003**, *15*, 2854−2860.
(46) Subramanian, V.; Wolf, E. E.; Kamat, P. V. *J. Am. Chem. Soc.* **2004**, *126*, 4943−4950.

Scheme 2. Linking CdSe QDs to TiO_2 Surface with a Bifunctional Surface Modifier

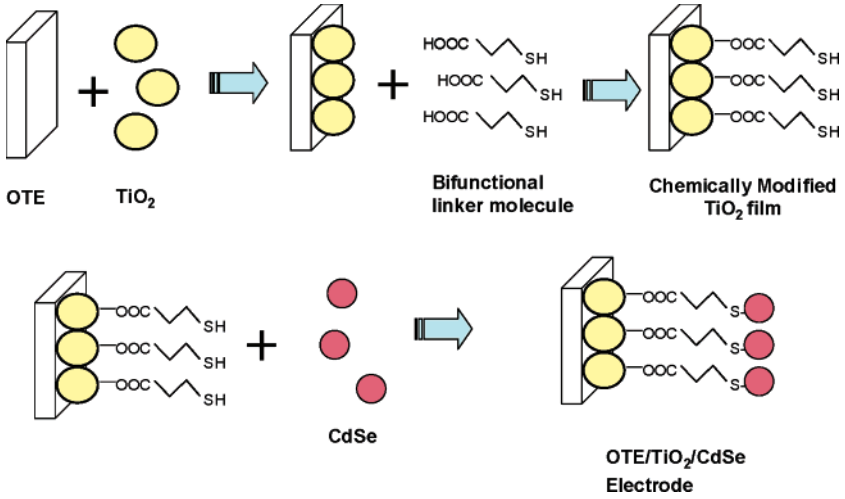

couple to maintain the stability of the CdSe QDs. The role of polysulfide electrolytes in maintaining the stability of metal chalcogenide semiconductors has been discussed elsewhere.[47−50] Both a Princeton Applied Research (PAR) model 173 potentiostat and a model 175 universal programmer were used to record $I-V$ characteristics. Photocurrent and open-circuit photovoltages (V_{oc}) were measured using a Keithley 617 programmable electrometer along with collimated, filtered light from an Oriel 450 W xenon arc lamp. A Bausch and Lomb high-intensity grating monochromator was introduced into the light path to select the excitation wavelength during IPCE measurements. All experiments were carried out under ambient conditions.

Femtosecond Transient Absorption Spectroscopy. Ultrafast transient absorption experiments were conducted using a Clark-MXR 2010 laser system and an optical detection system provided by Ultrafast Systems (Helios). The source for the pump and probe pulses is the fundamental of the Clark laser system (775 nm, 1 mJ/pulse, fwhm = 130 fs, 1 kHz repetition rate). A second harmonic generator is introduced into the path of the laser beam to provide 387 nm (3.20 eV, 130 fs) laser pulses for the pump. 95% of the fundamental is used to generate the second harmonic, while 5% of the output is used to generate a white light continuum. Prior to creating the white light probe, the fundamental is fed through a delay line providing an experimental time window of 1.6 ns with a maximum step resolution of 7 fs. The pump beam is attenuated to 5 μJ/pulse with a spot size of 2 mm (diameter) at the sample where it is merged with the white light incident on the sample cell with an angle <10°. After passing through the 2 mm cell, the probe is focused onto a 200 μm core fiber connected to a CCD spectrograph (Ocean Optics, S2000-UV−vis), enabling time-resolved spectra to be recorded (425−800 nm). Typically, 5000 excitation pulses are averaged to obtain the transient spectrum at a set delay time. Kinetic traces at appropriate wavelengths are assembled from the time-resolved data. All measurements were conducted at room temperature.

Results and Discussion

Optical Properties. Figure 1 shows the absorption and emission spectra of CdSe QDs in toluene. The particles exhibit transitions in the visible with a sharp band edge absorption at 550 nm (~2.25 eV). By comparing this spectrum to the sizing

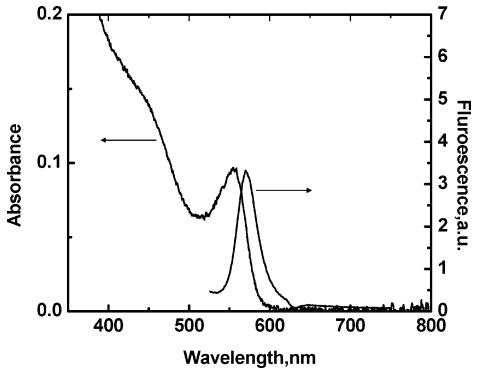

Figure 1. Absorbance and emission spectra of CdSe QDs in toluene. Emission spectrum was recorded using 410 nm excitation.

curve reported by Peng and co-workers,[45] we obtain a particle diameter of ~3 nm. The CdSe particles also exhibit band edge emission at 570 nm (~2.17 eV). The TiO_2 particles employed in our studies are large band gap semiconductors, which absorb UV light with an onset at 360 nm (~3.44 eV). They have diameters between 40 and 50 nm. The large corresponding surface area enables many smaller CdSe QDs to be linked to a single TiO_2 particle, facilitating interparticle electron transfer. The lower-lying conduction band of TiO_2 (−0.5 V vs NHE) as compared to CdSe (≤−1.0 V vs NHE) minimizes charge recombination and also rectifies any charge transport.[19, 34]

Linking of CdSe Particles with TiO_2 Using a Bifunctional Surface Modifier. Bifunctional linker molecules (HOOC−R−SH) with carboxylate and thiol functional groups facilitate binding CdSe QDs to TiO_2. Such an approach has been used to successfully link TiO_2 nanoparticles to CdS[51−53] as well as to gold nanoparticles.[54,55] In the present study, we have chosen three linker molecules of varying chain length, mercaptopropionic acid (MPA), thiolacetic acid (TAA), and mercaptohexadecanoic acid (MDA). The THF solution containing HOOC−

(47) Tenne, R. *J. Electroanal. Chem. Interfacial Electrochem.* **1983**, *143*, 113−20.
(48) Ueno, Y.; Minoura, H.; Nishikawa, T.; Tsuiki, M. *J. Electrochem. Soc.* **1983**, *130*, 43−7.
(49) Mueller, N. T., R.; Cahen, D. *J. Electroanal. Chem. Interfacial Electrochem.* **1981**, *130*, 373−9.
(50) Liu, C. J.; Olsen, J.; Saunders, D. R.; Wang, J. H. *J. Electrochem. Soc.* **1981**, *128*, 1224−8.
(51) Lawless, D.; Kapoor, S.; Meisel, D. *J. Phys. Chem.* **1995**, *99*, 10329−10335.
(52) Granot, E.; Patolsky, F.; Willner, I. *J. Phys. Chem. B* **2004**, *108*, 5875−5881.
(53) Baron, R.; Huang, C. H.; Bassani, D. M.; Onopriyenko, A.; Zayats, M.; Willner, I. *Angew. Chem., Int. Ed.* **2005**, *44*, 4010−4015.
(54) Kamat, P. V.; Barazzouk, S.; Hotchandani, S. *Angew. Chem., Int. Ed.* **2002**, *41*, 2764−2767.
(55) Zayats, M.; Kharitonov, A. B.; Pogorelova, S. P.; Lioubashevski, O.; Katz, E.; Willner, I. *J. Am. Chem. Soc* **2003**, *125*, 16006−16014.

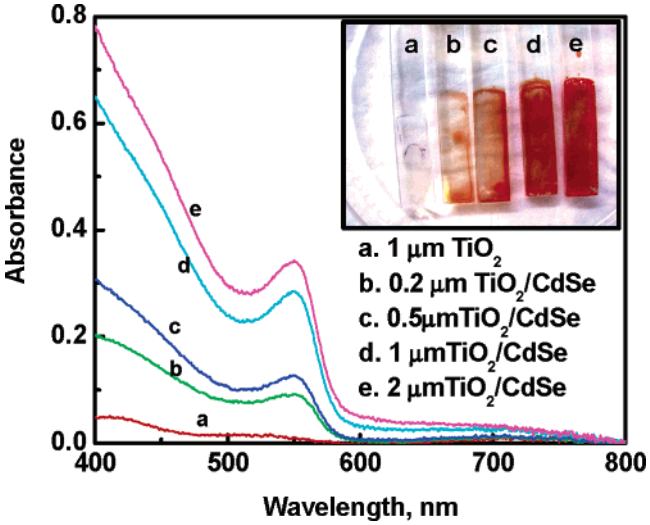

Figure 2. Absorption spectra of the OTE/TiO_2 films linked with CdSe QDs using MPA as a linker. Spectrum a corresponds to blank TiO_2 film before modification. Spectra b−e correspond to the OTE/TiO_2/MPA/CdSe electrodes after modification with CdSe QDs. The TiO_2 film thickness was varied: (b) 0.2 μm, (c) 0.5 μm, (d) 1 μm, and (e) 2μm. The photograph of these films is shown in the inset.

R−SH is added dropwise to a stirred CdSe suspension in THF:EtOH (1:1). CdSe nanoparticles undergo ligand exchange with HOOC−R−SH through the thiol linkage. Controlled amounts of titanium isopropoxide hydrolyzed in 1:1 THF:EtOH are added dropwise to the surface modified CdSe nanoparticles. The resulting suspensions are then examined using transient absorption spectroscopy.

Modification of the TiO_2 film with HOOC−R−SH was carried out by immersing the OTE/TiO_2 electrode in an acetonitrile-based HOOC−R−SH solution for 4 h. The electrode was washed thoroughly with acetonitrile and then immersed in a toluene suspension of CdSe QDs. TiO_2 has a strong affinity for the carboxylate group of the linker molecules, as demonstrated previously with a variety of sensitizing dyes.[56,57] Thiol and amine groups, on the other hand, bind strongly to CdSe nanoparticles.[58−63] Scheme 2 illustrates the principle behind anchoring CdSe QDs onto a nanostructured TiO_2 film.

Absorption spectra, recorded after linking CdSe QDs to MPA-prefunctionalized TiO_2 films with different thicknesses, are shown in Figure 2. The similarity of the resulting film's absorbance to that of QDs in solution (Figures 1 and 2) shows that the nanocrystals retain their optical properties when bound to TiO_2. Specifically, both the absorption onset and the band edge peak of the CdSe QDs are unaffected as a result of their binding to the mesoporous TiO_2 film. Once the deposition is complete, subsequent exposure of the films to CdSe suspensions causes no further increase in their absorbance. These observations suggest monolayer/submonolayer binding of CdSe QDs to TiO_2. Evidence for monolayer coverages is also obtained from the dependence of the CdSe absorbance on the TiO_2 film thickness (Figure 2). In particular, increasing the thickness of the TiO_2 film causes a corresponding increase in the CdSe absorbance. This can be seen visually from the colored electrodes in the photograph inset of Figure 2, which shows progressively darker CdSe films.

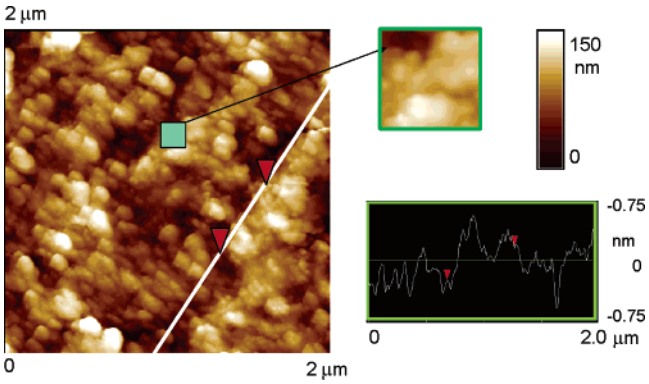

Figure 3. AFM image of an OTE/TiO_2/MPA/CdSe composite.

The increased absorbance can be understood as a consequence of the larger number of binding sites available for CdSe QDs within thicker TiO_2 films. Specifically, the porous TiO_2 matrix has interior surfaces on which CdSe QDs can bind provided that they penetrate the mesoporous network. The linear increase in the CdSe absorbance supports this and parallels the behavior of organic dye sensitizers commonly used to modify TiO_2 films. By contrast, a linear dependence of the CdSe absorbance with TiO_2 thickness is not expected if the QDs are deposited exclusively at the surface of the TiO_2 film. Thus, one can anchor CdSe QDs onto both exterior and interior surfaces of mesoscopic TiO_2 films through molecular linkers. Both TAA and MPA linkers provide better coverages of CdSe QDs on TiO_2 than MDA, suggesting that short chain linkers are better suited for this purpose. Control experiments, carried out in the absence of linker molecules, show inefficient binding of CdSe QDs to the TiO_2 film. Absorption spectra of CdSe QDs deposited on TiO_2 using different linker molecules are shown in the Supporting Information (Figure S1 in the Supporting Information).

Surface Characterization of the TiO_2 Films Modified with CdSe QDs. A tapping mode AFM image of CdSe particles linked to a TiO_2 film (OTE/TiO_2/MPA/CdSe) is shown in Figure 3. The morphology, consisting of the three-dimensional assembly of larger and smaller particles, is apparent from the surface topography. A magnified view highlights the presence of smaller CdSe nanoparticles on the TiO_2 surface. Further evidence comes from a cross sectional analysis, yielding average diameters of 50 ± 10 and 4 ± 1 nm for TiO_2 and CdSe nanoparticles, respectively. This is consistent with independent TEM sizing measurements. TiO_2 nanoparticles therefore provide the necessary foundation for anchoring smaller CdSe QDs via molecular linkers. Furthermore, the mesoscopic morphology of the TiO_2 film facilitates penetration of the 3 nm diameter CdSe QDs through pores in the matrix, enabling their uniform binding to both interior and exterior TiO_2 surfaces.

(56) Nazeeruddin, M. K.; Kay, A.; Rodicio, I.; Humphry, B. R.; Mueller, E.; Liska, P.; Vlachopoulos, N.; Graetzel, M. *J. Am. Chem. Soc.* **1993**, *115*, 6382−90.
(57) Meyer, T. J.; Meyer, G. J.; Pfennig, B. W.; Schoonover, J. R.; Timpson, C. J.; Wall, J. F.; Kobusch, C.; Chen, X. H.; Peek, B. M.; Wall, C. G.; Ou, W.; Erickson, B. W.; Bignozzi, C. A. *Inorg. Chem.* **1994**, *33*, 3952−3964.
(58) Rogach, A. L.; Kornowski, A.; Gao, M.; Eychmüller, A.; Weller, H. *J. Phys. Chem. B* **1999**, *103*, 3065−3069.
(59) Hens, Z.; Tallapin, D. V.; Weller, H. *Appl. Phys. Lett.* **2002**, 81, 4245−4247.
(60) Cassagneau, T.; Mallouk, T. E.; Fendler, J. H. *J. Am. Chem. Soc.* **1998**, *120*, 7848−7859.
(61) Landes, C.; Burda, C.; Braun, M.; El-Sayed, M. A. *J. Phys. Chem. B* **2001**, *105*, 2981−2986.
(62) Landes, C. F.; Braun, M.; El-Sayed, M. A. *J. Phys. Chem. B* **2001**, *105*, 10554−10558.
(63) Sharma, S.; Pillai, Z. S.; Kamat, P. V. *J. Phys. Chem. B* **2003**, *107*, 10088−10093.

Table 1. Kinetic Parameters of the Transient Bleach Recovery for the CdSe−MPA and CdSe−MPA−TiO_2 Systems[a]

	A_1	τ_1, ps	A_2	τ_2, ps	A_3	τ_3, ps
CdSe−MPA	−0.11 ± 0.003	14 ± 0.8	−0.13 ± 0.01	409 ± 62	−0.73 ± 0.01	7110 ± 700
CdSe−MPA−TiO_2	−0.21 ± 0.005	3.74 ± 0.18	−0.27 ± 0.005	103 ± 5	−0.48 ± 0.005	1870 ± 36

[a] Kinetic traces of Figure 6 were fitted using the three-exponential form $A_1 \exp(-t/\tau_1) + A_2 \exp(-t/\tau_2) + A_3 \exp(-t/\tau_3)$.

Transient Absorption Studies. Suspensions of CdSe QDs prepared in THF:EtOH (1:1) and capped with CdSe QDs (3 nm in diameter) were subjected to laser pulse excitation in a femtosecond pump−probe spectrophotometer. The transient spectra were recorded at different delay times following the laser pulse excitation. Figure 4 shows the time-resolved bleaching of the MPA capped CdSe suspension. The difference absorption (bleaching) maxima observed at 440 and 530 nm confirm the disappearance of CdSe absorption immediately following the laser pulse excitation. The formation of excitonic states within the CdSe cluster causes the changes in the absorption spectrum.[64]

The steady-state absorption spectrum of the CdSe QDs (∼3 nm diameter) is also shown in Figure 4 for reference. The two broad peaks around 440 and 530 nm in the ground-state absorption are attributed to transitions into s- ($1S_{3/2}1S_e$) and p-like ($1P_{3/2}1P_e$) states.[65−67] The distinct difference between the two spectral bands allows us to follow these two excited states by monitoring the bleaching at the corresponding wavelengths, 440 and 530 nm, respectively.

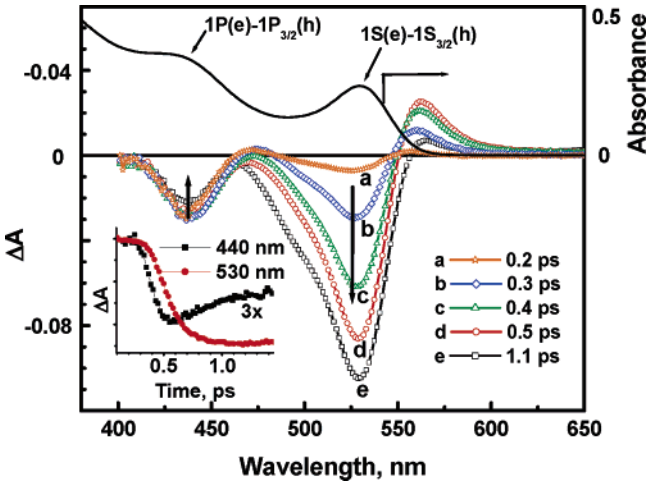

Figure 4. Top: Absorption spectrum of MPA capped CdSe colloids in THF/EtOH. Bottom: Time-resolved difference absorption spectra recorded following 387 nm laser pulse excitation of MPA capped CdSe suspension. Inset: Short time-scale kinetic traces of the s and p states.

Ultraband gap excitation induced by the laser pulse (387 nm) creates high-energy excitonic states, which quickly undergo intraband relaxation. The 440 and 530 nm transient absorption profiles (inset in Figure 4) highlight the relaxation of the higher energy state into the s-state. Formation of the p-like ($1P_{3/2}1P_e$) state is completed within the laser pulse duration of 130 fs. Quick relaxation in ∼1 ps results in the population of a lower energy s-like ($1S_{3/2}1S_e$) state with an increased bleaching at 530 nm. The 530 nm bleach (inset of Figure 4) reaches a maximum during the first 2 ps following the laser pulse excitation. The transient bleaching observed at these early times further reflects the charge separation achieved in the CdSe QDs. A major fraction of this bleaching recovers in the nanosecond time scale as the photogenerated electrons and holes recombine or undergo trapping.[67−70] The kinetics of this recovery is complex and can be analyzed by a three-exponential kinetic fit. The decay parameters are given in Table 1. The longer survivability of electrons and holes as charge separated pairs paves the way for attaining charge transfer at the interface.

Charge Injection into TiO_2 Particles. To probe the interparticle electron transfer between excited CdSe and TiO_2, we compared the transient bleaching recovery in the absence and presence of colloidal TiO_2. Note that in both of these experiments the surface of CdSe was capped with MPA and maintains similar surface trapping dynamics in both cases. Figure 5A compares the ground-state absorption and emission of CdSe and CdSe−TiO_2 particle suspensions. The CdSe absorption in the visible remains unchanged by the addition of TiO_2 colloids. The TiO_2 absorption can only be seen at wavelengths below 360 nm. The absorption at the pump wavelength (387 nm) is also similar in both cases, thus ensuring the selective excitation of CdSe in both cases. To avoid Auger-recombination of charge carriers, the pump fluence was kept at low levels (∼230 μJ/cm^2), resulting in an average excitation level of ∼0.3 electron−hole pairs per CdSe QD (absorption cross section ∼7×10^{-16} cm^2 at 387 nm). The emission spectra recorded upon addition of TiO_2 to colloidal CdSe show a decrease of the emission yield by about 80% with no noticeable changes in the spectral characteristics. These results indirectly support the hypothesis that the TiO_2 colloids are able to interact with excited CdSe particles with a mechanism similar to the electron-transfer process proposed in earlier transient absorption studies with CdS colloids.[71−73]

The transient absorption spectra representing the bleaching recovery of the MPA capped colloids were recorded in the absence (Figure 5B) and presence of TiO_2 colloids (Figure 5C). In the absence of TiO_2, the bleaching of the recovery of the 530 nm band occurs slowly, and only about 30% of the bleaching is recovered in 1.5 ns. On the other hand, the presence of TiO_2 in the suspension accelerates the recovery and nearly 75% of the recovery is seen in 1.5 ns. The enhanced recovery of the 530 nm band reflects the influence of TiO_2 in accepting electrons from the relaxed $1S_{3/2}1S_e$ state. Because of the limitations of the pulse width of the pump laser, we were not able to resolve the interactions with the $1P_{3/2}1P_e$ state.

(64) Hilinski, E. F.; Lucas, P. A.; Wang, Y. *J. Chem. Phys.* **1988**, *89*, 3435−3441.
(65) Norris, D. J.; Efros, A. L.; Rosen, M.; Bawendi, M. G. *Phys. Rev. B* **1996**, *53*, 16347−16354.
(66) Norris, D. J.; Bawendi, M. G. *Phys. Rev. B* **1996**, *53*, 16338−16346.
(67) Klimov, V. I. *J. Phys. Chem. B* **2000**, *104*, 6112−6123.
(68) Burda, C.; Green, T. C.; Link, S.; El-Sayed, M. A. *J. Phys. Chem. B* **1999**, *103*, 1783−1788.
(69) Mohamed, M. B.; Burda, C.; El-Sayed, M. A. *Nano Lett.* **2001**, *1*, 589−593.
(70) Braun, M.; Burda, C.; Mohamed, M.; El-Sayed, M. *Phys. Rev. B* **2001**, 6403, art. no.-035317.
(71) Evans, J. E.; Springer, K. W.; Zhang, J. Z. *J. Chem. Phys.* **1994**, *101*, 6222−6225.
(72) Gopidas, K. R.; Bohorquez, M.; Kamat, P. V. *J. Phys. Chem.* **1990**, *94*, 6435−40.
(73) Sant, P. A.; Kamat, P. V. *Phys. Chem. Chem. Phys.* **2002**, *4*, 198−203.

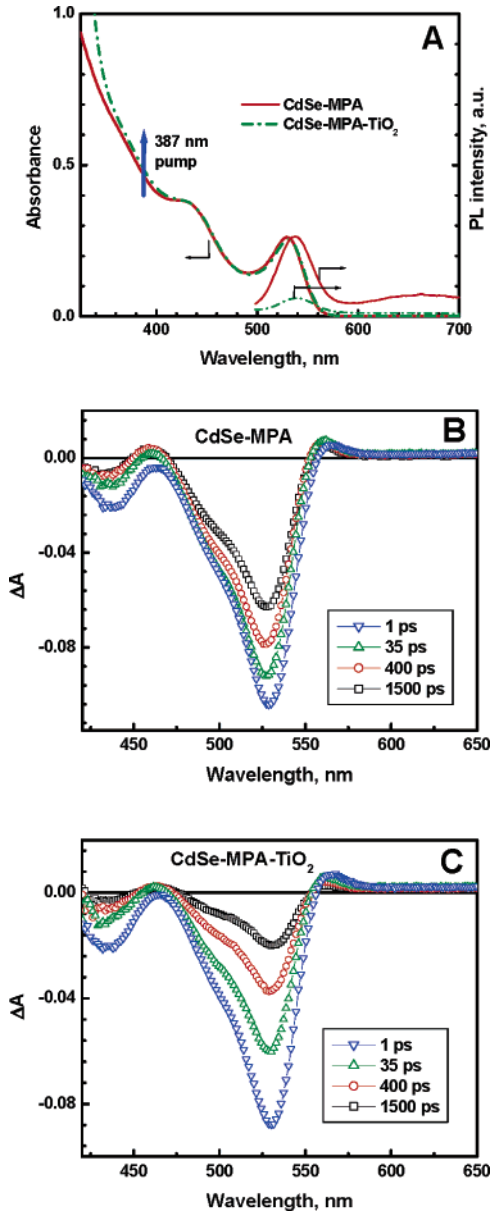

Figure 5. (A) Absorption and emission spectra of MPA capped CdSe colloids before and after mixing with colloidal TiO_2 particles. (B) and (C) represent bleaching recovery of MPA capped CdSe QDs in the absence and presence of TiO_2 colloids, respectively. Excitation was at 387 nm.

The recovery of the transient bleaching was multiexponential. The kinetic analysis using three-exponential fits of the absorption profiles is shown in Figure 6, and the parameters are summarized in Table 1. It has been demonstrated earlier that the transient bleaching is a measure of charge separation and the production of one or two electron−hole pairs can completely bleach the excitonic absorption of a semiconductor particle. Thus, disruption of the electron−hole pair by the transfer of electrons to TiO_2 is expected to increase the rate of the bleaching recovery.[64] These decreased lifetimes therefore reflect the participation of excited CdSe in injecting electrons into TiO_2 (eqs 1 and 2).

$$\mathrm{CdSe} + h\nu \rightarrow \mathrm{CdSe}\,(e_p + h_p) \rightarrow \mathrm{CdSe}\,(e_s + h_s) \quad (1)$$

$$\mathrm{CdSe}\,(e_s) + \mathrm{TiO_2} \rightarrow \mathrm{CdSe} + \mathrm{TiO_2}(e) \quad (2)$$

We estimated the rate constant for the electron transfer from the relaxed $1S_{3/2}1S_e$ state (reaction 1) by comparing the

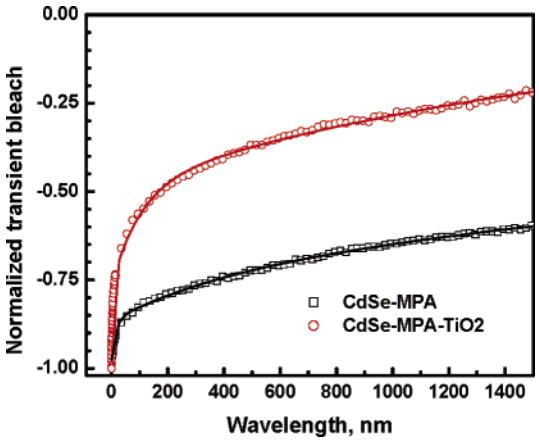

Figure 6. Long time-scale absorption recovery profiles at 530 nm recorded following the 387 nm laser pulse excitation of CdSe−MPA and CdSe−MPA−TiO_2.

Scheme 3. Deactivation of the Excited Electrons from the p- and s-States in CdSe QDs

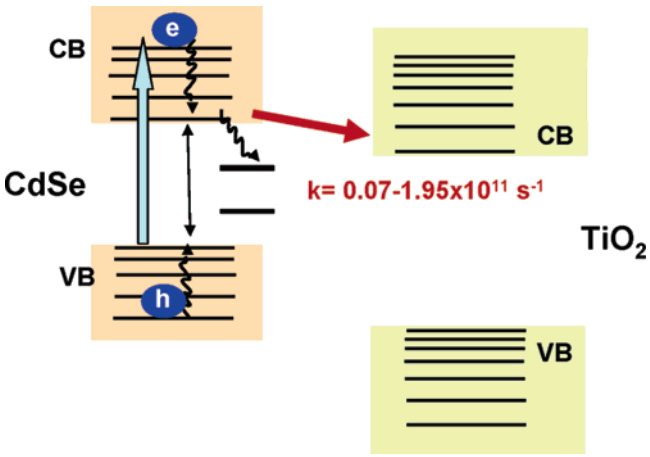

bleaching recovery lifetimes in the presence and absence of TiO_2. Because the first two lifetimes correspond to the major recovery in CdSe−TiO_2, we used these values for our estimate of the electron-transfer rate constant. If we assume that the observed decrease in lifetime arises from charge transfer into TiO_2, we can determine the charge-transfer rate constant through the following expression

$$k_{et} = 1/\tau_{(\mathrm{CdSe+TiO_2})} - 1/\tau_{(\mathrm{CdSe})} \quad (3)$$

Using the lifetimes values of 14.0 ps and 409.0 (CdSe) and 3.74 ps and 103.0 (CdSe−TiO_2) obtained for the recovery of the 530 nm, we obtain rate constants in the range of (0.073−1.95) × 10^{11} s^{-1}. These values represent the range of rate constants at which electron injection into TiO_2 occurs from the thermally relaxed excited state (Scheme 3). Although the possibility exists for hot electron injection from the higher energy p-state for both InP[74] and CdSe,[68] we were not able to resolve its contribution in the present experiments because of pulse width limitations. (See Supporting Information Figure S2 for the comparison of traces at 440 nm.) Factors such as the heterogeneity of the surface, interparticle interactions, and the accessibility of injection sites contribute to the complex

(74) Rosenwaks, Y.; Thacker, B. R.; Nozik, A. J.; Ellingson, R. J.; Burr, K. C.; Tang, C. L. *J. Phys. Chem.* **1994**, *98*, 2739−2741.

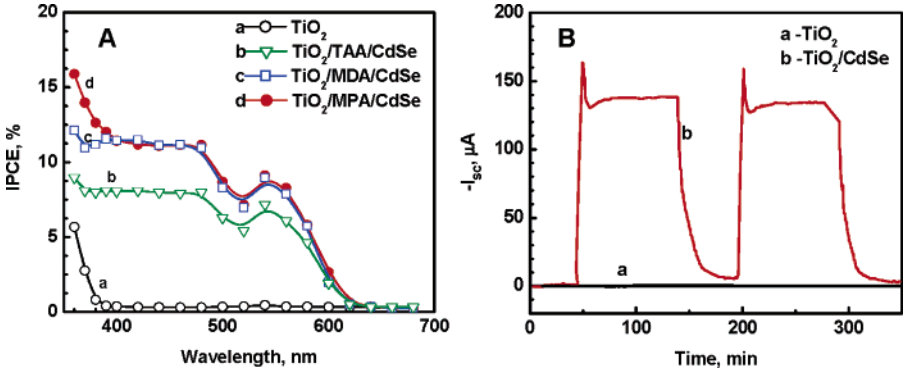

Figure 7. (A) Photocurrent action spectra of TiO_2 (a), and OTE/TiO_2/L/CdSe films where L = (b) TAA, (c) MDA, and (d) MPA. Electrolyte 0.1 M Na_2S and Pt counter electrode. (B) Photocurrent versus time profiles of (a) OTE/TiO_2 and (b) OTE/TiO_2/CdSe films using MPA as a linker molecule (0.2 M Na_2S electrolyte and illumination intensity = 120 mW/cm^2).

charge injection kinetics. Aiding the interparticle electron transfer are vacant energy levels in the TiO_2 that facilitate direct, subpicosecond−nanosecond electron transfer from excited sensitizers.[75−78]

Photoelectrochemistry of OTE/TiO_2/CdSe Films. In a pioneering study, Gerischer and co-workers[13] demonstrated that semiconductors such as CdS, which absorb in the visible, are capable of injecting electrons into TiO_2 films. Based on the principle of sensitizing large band gap with smaller band gap semiconductors, efforts have been made to employ CdSe and PbS[16] as sensitizers to extend the photoresponse of TiO_2 into the visible. Composite semiconductor systems with suitably matched energetics facilitate charge rectification, minimizing charge recombination. In the present work, we have probed the photoelectrochemical behavior of TiO_2 films modified with CdSe QDs in a three-arm cell with a Pt gauze counter electrode and a saturated calomel electrode (reference). A Na_2S solution serves as the regenerative redox couple. Upon illumination of the OTE/TiO_2/CdSe film with visible light, an anodic current is generated. An open-circuit voltage of 0.5 V and short circuit current of 0.14 mA are also obtained.

The open-circuit potential is independent of the TiO_2 film thickness, unlike the short circuit current (see Table S1 in the Supporting Information), which varies from 0.12 to 0.145 mA/cm^2 when the thickness of the TiO_2 film increases from 0.2 to 2 μm. In all cases, larger amounts of CdSe in thicker films yield higher photocurrents. These observations show that CdSe is a major contributor to the observed photocurrent. Control experiments, carried out with TiO_2 electrodes alone, do not exhibit any photoresponse in the visible.

The photoelectrochemical response of the TiO_2/CdSe films was further analyzed by measuring their action spectra. Figure 7 shows the photoresponse of the TiO_2 film before and after modification with CdSe QDs. TiO_2/CdSe films prepared using different linker molecules were also compared. The incident photon to current conversion efficiency (IPCE) at different wavelengths was determined from the short circuit photocurrents

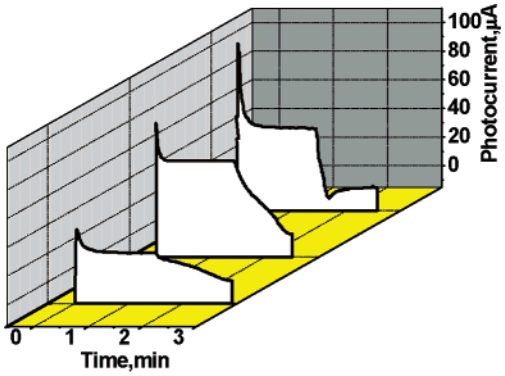

Figure 8. Effect of Na_2S electrolyte concentration on the photocurrent generation using an OTE/TiO_2/MPA/CdSe electrode (Pt wire counter electrode; illumination intensity of 120 mW/cm^2).

Scheme 4. Charge Injection, Charge Transport, and Charge Recombination Following Visible Light Excitation of CdSe QDs Assembled on OTE/TiO_2 Electrode at (A) Low and (B) High Excitation Intensities

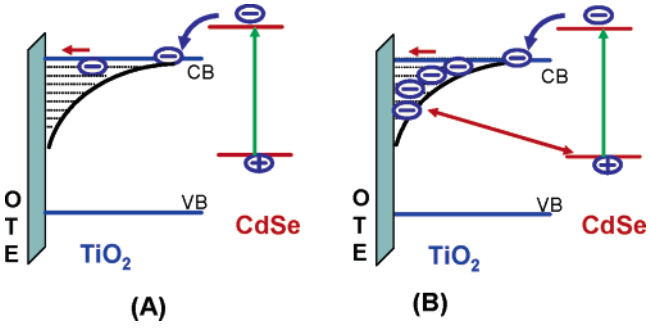

(I_{sc}) monitored at different excitation wavelengths (λ) using the expression

$$\text{IPCE\%} = [1240 \times I_{sc}\ (\text{A/cm}^2)]/[\lambda\ (\text{nm}) \times I_{inc}(\text{W/cm}^2)] \times 100 \quad (4)$$

where I_{inc} is the incident light power. The spectral response of the IPCE spectrum of TiO_2/CdSe films closely matches the absorption spectrum recorded in Figure 2. All three TiO_2/CdSe films show photocurrent responses below 600 nm in contrast with the TiO_2 film that responds only in the UV (<380 nm). A maximum IPCE value of 12% was observed for TiO_2 films modified with CdSe QDs using MDA and MPA as linker molecules. IPCE values of CdSe/TiO_2 films prepared using TAA linker molecules show slightly lower efficiencies with a

(75) Ramakrishna, S.; Willig, F. *J. Phys. Chem. B* **2000**, *104*, 68−77.
(76) Trachibana, Y.; Haque, S. A.; Mercer, I. P.; Durrant, J. R.; Klug, D. R. *J. Phys. Chem. B* **2000**, *104*, 1198−1205.
(77) Randy, J.; Ellingson, R. J.; Asbury, J. B.; Ferrere, S.; Ghosh, H. N.; Sprague, J. R.; Lian, T.; Nozik, A. J. *J. Phys. Chem. B* **1998**, *102*, 6455−6458.
(78) Gaillard, F.; Sung, Y.-E.; Bard, A. J. *J. Phys. Chem. B* **1999**, *103*, 667−674.

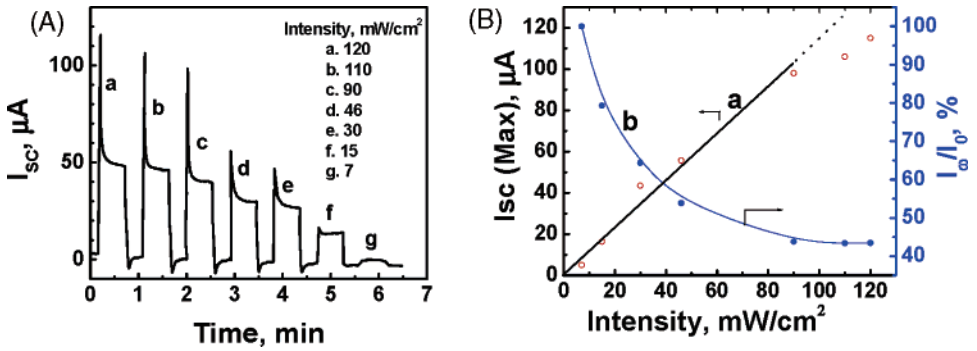

Figure 9. (A) Effect of excitation intensity on the stability of photocurrent generation following the visible excitation (>400 nm) of OTE/TiO_2//CdSe electrode. Na_2S concentration was 0.1 M Na_2S. Excitation intensity was maintained at (a) 120 mW/cm^2, (b)110 mW/cm^2, (c) 90 mW/cm^2, (d) 46 mW/cm^2, (e) 30 mW/cm^2, (f) 15 mW/cm^2, and (g) 7mW/cm^2. (B) Dependence of maximum photocurrent (I_0) and the ratio of stabilized photocurrent to maximum photocurrent (I_∞/I_0) on the excitation intensity.

maximum IPCE of 9%. These lower IPCE values indicate that a larger fraction of carriers are lost to charge recombination within the particle or at the CdSe/TiO_2 interface. Comparison of the three traces (b, c, and d in Figure 7A) indicates that MPA and MDA are better than TAA as linkers for anchoring CdSe QDs to TiO_2. Unless stated otherwise, the remaining experiments were therefore performed with MPA as the linker molecule.

Upon visible light illumination (λ > 400 nm), TiO_2/CdSe films show a prompt rise in both photocurrent and photovoltage. The photovoltage remains steady and attains saturation at intensities greater than 50 mW/cm^2 (Figure S3B in the Supporting Information). However, a sharp decrease in the short circuit current is seen, within the first 30 s of illumination, before stabilizing (Figure 7B). This trend of the photocurrent decaying in the initial seconds of illumination can be seen during repeated on−off cycles of illumination. By contrast, in most photoelectrochemical cells employing nanostructured TiO_2 or dye sensitized TiO_2 films, a steady photocurrent is immediately obtained following excitation of the sample. The reason for the observed photocurrent decay during the initial excitation period arises from one of two reasons: (i) the inability of the redox couple to quickly scavenge photogenerated holes or (ii) dominant charge recombination/scattering at the CdSe/TiO_2 heterointerface or at grain boundaries within the mesoporous TiO_2 network.

If the scavenging of holes is a limiting factor, we can overcome this effect by increasing the concentration of the redox couple. To assess this possibility, the photocurrent evolution and its initial decay were recorded during on−off illumination cycles by varying the Na_2S concentration from 0.005 to 0.05 M (Figure 8). As expected, the maximum photocurrent, observed immediately upon illuminating the TiO_2/CdSe film, increases with increasing concentration of Na_2S. The increased rate of hole scavenging at the CdSe−electrolyte interface reduces charge recombination. However, the initial decay becomes more predominant at higher concentrations of Na_2S. The fact that we continue to observe the decay of the photocurrent at high Na_2S concentrations rules out inefficient hole scavenging as the origin of the observed effect.

To see whether the increased concentration of charge carriers contributes to recombination losses/scattering at heterointerfaces and internal grain boundaries, we varied the excitation intensity. The photocurrent response to illumination is shown in Figure 9A. Because the production of charge carriers increases linearly with the incident light intensity, we expect the magnitude of the photocurrent to scale similarly. However, if we fail to transport these photogenerated electrons to the collecting electrode, a deviation in this photocurrent behavior will occur. Indeed, the maximum photocurrent seen immediately after illuminating the TiO_2/CdSe film scales linearly with excitation intensity (Figure 9B). Deviations from linearity at higher intensities (>70 mW/cm^2) arise from saturation effects.

The decay of the photocurrent at early times occurs predominantly at high excitation intensities. Conversely, the photocurrent obtained at low excitation intensities is remarkably stable. The fraction of the stable current, as measured by the ratio of the current at long times to its maximum value (I_∞/I_0), is plotted as a function of excitation intensity in Figure 9B. At low intensities, we harvest nearly 100% of the electrons injected into TiO_2. As more charge carriers are generated, this value decreases such that, at high excitation intensities, only ~40% of the charge carriers are collected. This can be understood as follows. At low intensities, few electrons are injected into TiO_2. These electrons are transported to the OTE surface with little loss arising from scattering or charge recombination at either the CdSe/TiO_2 interface or the internal TiO_2 grain boundaries. With increasing excitation intensity, more electrons are injected into TiO_2. Because the injection of electrons into TiO_2 is an ultrafast process (femtosecond−picosecond time scale) and transport of electrons across the nanostructured film is relatively slow, occurring on the microsecond−millisecond time scale, electrons begin to accumulate within the mesoporous TiO_2 network. The trapping of electrons at Ti^{4+} sites has been extensively studied; up to 200 electrons can be stored within the shallow and deep traps of a single TiO_2 particle.[46,79] As electrons accumulate within the TiO_2 matrix, the probability that subsequently injected carriers undergo scattering and/or recombination at the CdSe/TiO_2 heterointerface and at internal TiO_2 grain boundaries increases. This causes the fraction of carriers harvested to decrease and explains why the charge harvesting efficiency of the cell decreases with increasing excitation intensity. Scheme 4 shows the electron accumulation at two different excitation intensities. Suppressed electron transport in the TiO_2/CdSe composite therefore restricts optimal performance of the cell at higher light intensities and shows that the charge-transport across the TiO_2 film is a major limiting factor in CdSe QD-based solar cells.

(79) Rothenberger, G.; Moser, J.; Graetzel, M.; Serpone, N.; Sharma, D. K. *J. Am. Chem. Soc.* **1985**, *107*, 8054−9.

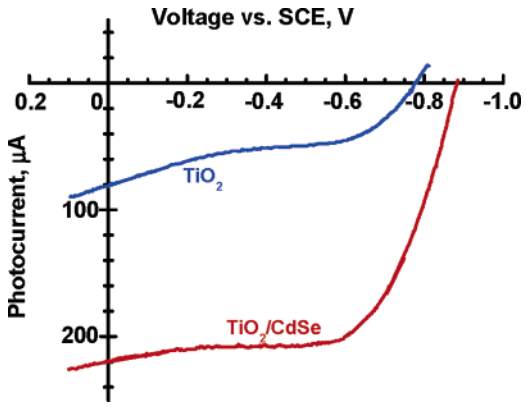

Figure 10. *I*−*V* characteristics of (a) OTE/TiO_2 and (b) OTE/TiO_2/MPA/CdSe films. Electrolyte 0.1 M Na_2S. The filtered lights allowed excitation of TiO_2 and CdSe films at wavelengths greater than 300 and 400 nm, respectively.

One approach to facilitating electron transport in nanostructured semiconductor films involves applying a positive bias to the working electrode. The photocurrent generated at different applied potentials for OTE/TiO_2 and OTE/TiO_2/CdSe electrodes is shown in Figure 10. Excitation of TiO_2 and TiO_2/CdSe films was carried out using light with wavelengths greater than 300 and 400 nm, respectively. Both films show anodic photocurrents when subjected to band gap excitation. The observed photocurrents increase as the potential is swept toward positive values. At potentials greater than −0.6 V vs SCE, the anodic photocurrent saturates at which point electron transport is no longer a limiting factor. The potential at which we observe zero current is a measure of the flat band potential and reflects the maximum attainable open-circuit voltage. We observe zero current at potentials of −0.78 and −0.88 V vs SCE for TiO_2 and TiO_2/CdSe films, respectively. The 100 mV shift represents the improved energetics of the TiO_2/CdSe films and shows the advantage of using composite nanostructures for boosting open-circuit potentials.

Conclusions

Bifunctional organic molecules have been successfully employed to link two semiconductor nanostructures with tailored band offsets. Whereas the absorption properties of the QDs remain unchanged, the emission yield decreases dramatically when linked to the TiO_2 substrate. By combining spectroscopic and photoelectrochemical techniques, we have demonstrated the possibility of employing CdSe QDs for sensitizing TiO_2 particles and films. Electrons from the conduction band of CdSe are injected into TiO_2 particles with rate constants in the $(0.073-1.95) \times 10^{11}$ s^{-1} range. The photocurrent generation observed upon visible light excitation of CdSe QDs highlights the feasibility of their use as light harvesting antennae. At higher incident light intensities, scattering as well as recombination at internal grain boundaries due to the accumulation of carriers within TiO_2 dominates, causing the photocurrent to decrease. These studies point out the need for further improvement in the design of semiconductor QDs to maximize the photoconversion efficiency.

Acknowledgment. The research described herein was supported by the Department of Energy, Office of Basic Sciences. This is contribution number NDRL 4627 from the Notre Dame Radiation Laboratory.

Supporting Information Available: Complete ref 5, table illustrating the photovoltage and photocurrent at different TiO_2 thickness, absorption spectra of CdSe films obtained with different linkers, kinetic profiles of higher excited states in CdSe and CdSe/TiO_2, and photovoltage response. This material is available free of charge via the Internet at http://pubs.acs.org.

JA056494N